More than just a passive brick in the wall: the nucleosome facilitates DNA polymerase β activity in linker DNA and its PARP-dependent regulation in the BER pathway choice

Danil M. Shtanov [1,2], Tatyana A. Kurgina[1,2], Mikhail M. Kutuzov[1], Konstantin N. Naumenko[1], Alexander A. Ukraintsev[1], Nina A. Moor[1], Olga I. Lavrik[1]*

[1]Institute of Chemical Biology and Fundamental Medicine, SB RAS, Novosibirsk, Russia

[2] These authors contributed equally: Danil M. Shtanov and Tatyana A. Kurgina

*Corresponding author O. I. Lavrik, Email: lavrik@1bio.ru ORCID: https://orcid.org/0000-0001-5980-8889

Abstract

DNA polymerase β (Polβ) is a central player of base excision repair (BER), performing gap-filling synthesis on damaged DNA. While nucleosome core particles (NCPs) are known to impede activity of BER enzymes, the regulation of this process in linker DNA adjacent to nucleosomes remains unclear. Here we demonstrate an unexpected stimulation of Polβ-catalyzed gap-filling and strand-displacement synthesis in linker DNA by the adjacent NCP. Notably, the nucleosomal context reinforces the regulatory modulation of Polβ activity by PARP1/PARP2 and FEN1. While linker histone H1 restricts strand-displacement synthesis at the nucleosome entry/exit site, PARP1 and PARP2 modulate Polβ function through competitive binding to DNA gaps or nicks and via poly(ADP-ribosyl)ation (PARylation). At the same time, PARPs binding differentially regulates BER sub-pathway choice, and PARylation alleviates H1-mediated inhibition. These findings reveal a multi-layered regulatory system wherein the nucleosome acts as a dynamic platform coordinating Polβ activity and its interplay with chromatin-associated factors, influencing the balance between short- and long-patch BER. The research advances understanding of chromatin-mediated control of BER DNA repair synthesis and the functional specialization of PARP1 and PARP2 in maintaining genome stability.

Keywords

DNA repair, BER, nucleosome, PARP1, PARP2, H1, chromatin, SP-BER, LP-BER

Highlights

The nucleosome core particle acts not only as a barrier but also as a stimulator of Polβ-mediated DNA repair synthesis in adjacent linker DNA.

The nucleosome acts as an allosteric platform that enhances the regulatory functions of chromatin-associated factors (PARP1, PARP2, H1) in the linker DNA repair synthesis.

PARP1 suppresses overall Polβ synthesis, while PARP2 specifically inhibits strand displacement, thereby gating the choice between short- and long-patch BER pathways.

Introduction

DNA polymerase β (Polβ) is the primary DNA polymerase responsible for gap-filling synthesis during the base excision repair (BER) pathway[1,2]. This enzyme processes the central 1-nucleotide (nt) gap intermediate through two distinct activities: its polymerase domain catalyzes nucleotide insertion, while its N-terminal lyase (8-kDa) domain excises the 5'-deoxyribose phosphate (5'-dRP) moiety, enabling the short-patch (SP) BER sub-pathway. Polβ can also perform limited strand-displacement synthesis, a prerequisite for the alternative long-patch (LP) BER sub-pathway where 2-11 nucleotides are incorporated[3]. A defining biochemical feature of Polβ is its distributive mode of synthesis. Unlike processive replicative polymerases, Polβ does not remain tightly bound to its DNA template but instead dissociates after incorporating a short patch of 2-3 nucleotides[4]. However, this distributive kinetics also means that the overall efficiency of DNA synthesis is highly dependent on the enzyme's rebinding rate. The resulting flap is cleaved by flap endonuclease 1 (FEN1), which stimulates Polβ activity in strand-displacement synthesis, in accordance with the "passing the baton" mechanism [5–7]. Notably, the fidelity of Polβ decreases substantially during strand-displacement synthesis compared to single-nucleotide gap filling, highlighting the critical importance of regulating its catalytic choice between these two modes[8]. Overexpression of Polβ, as observed in certain malignancies, is thought to promote a shift towards the long-patch BER (LP-BER) pathway and, under specific conditions, may even facilitate its aberrant recruitment into the nucleotide excision repair (NER) pathway. Such misregulation ultimately contributes to increased mutation rates and genomic instability[9,10].

The progression and efficiency of BER are tightly regulated by various factors, prominently including poly(ADP-ribose) polymerases 1 and 2 (PARP1 and PARP2). These enzymes function as molecular sensors of DNA strand breaks, binding to damaged DNA and catalyzing the synthesis of poly(ADP-ribose) (PAR) chains[11]. PARylation serves as a signal for the recruitment of DNA repair factors but also modulates enzyme activity; for instance, automodification of PARP1 and PARP2 promotes their dissociation from DNA, thereby facilitating access for repair enzymes like Polβ[12–15]. PARP1 and PARP2 exhibit distinct affinities for different BER intermediates: PARP1 binds effectively to undamaged DNA, AP-sites, gaps and nicks, whereas PARP2 shows a marked preference for gapped and nicked DNAs[12,13,16,17]. Consequently, PARP1 influences all stages of BER[12,18], while PARP2 acts as a key regulator of final steps, including the handoff between Polβ and DNA ligase IIIα (LigIIIα)[14].

A critical layer of DNA repair regulation is added by the packaging of genomic DNA into chromatin. The nucleosome core particle (NCP), the fundamental repeating unit of chromatin, presents a significant structural barrier to DNA repair machinery[19]. Extensive biochemical and recent structural studies, comprehensively detailed in an excellent recent review[20], have demonstrated that the activities of DNA glycosylases, apurinic/apyrimidinic endonuclease 1 (APE1), Polβ, and LigIIIα are substantially suppressed on nucleosomal DNA compared to naked DNA[14,21–24]. The translational and rotational positioning of a DNA lesion within the nucleosome profoundly influences its accessibility to BER enzymes[25–28]. For example, the activity of Polβ in gap-filling synthesis within the nucleosome follows a strong position-dependent gradient, being most efficient near the entry/exit sites[25,29] or linker DNA[26]. Cryo-EM structures reveal that the reduced activity of Polβ in processing low-accessible lesions stems from the necessity for enzyme to engage in extensive "global DNA sculpting," displacing ~35 base pairs of DNA from the histone octamer to induce a ~90° DNA bend[29]. Similarly, ligation of the final nick by the XRCC1-LigIIIα complex is efficient only near the nucleosome periphery[23]. This constrained repair capacity within chromatin is biologically significant, as it correlates with elevated DNA repair efficacy and mutation rates in nucleosome-dense genomic regions *in vivo*[30–32].

To overcome the chromatin barrier, cells employ active chromatin remodeling strategies[33,34]. PARP1 and PARP2, in complex with the histone PARylation factor 1 (HPF1), play a pivotal role in this process by catalyzing PARylation of core histones, primarily on serine residues [35,36]. This HPF1-dependent histone PARylation triggers local chromatin relaxation facilitating the access of repair factors to lesions[37].

While histone PARylation may directly relax nucleosome structure to facilitate Polβ activity on nucleosomal substrates *in vitro*[38], its principal function *in vivo* is likely the targeted recruitment of chromatin remodelers[39–42]. ADP-ribosylation of histones in the vicinity of a nucleosomal DNA lesion, which is most efficiently catalyzed by PARP2[16,17,43], might serve as a signal to recruit ALC1. This remodeler would then catalyze nucleosome sliding away from the damage site, effectively repositioning the lesion into the more accessible linker DNA, where it becomes fully exposed to the repair machinery[42,44–46].

Whereas the mechanisms of BER within the nucleosome core have been increasingly elucidated, the repair landscape in linker DNA regions – the stretches connecting nucleosome cores – remains less characterized. The nucleosome itself imposes a strong bias for the SP-BER pathway, effectively limiting DNA repair synthesis within the nucleosome core to single-nucleotide insertion; this phenomenon is less pronounced in linker DNA[47].

It was previously established that Polβ-catalyzed strand-displacement synthesis in linker DNA produced a repair patch whose size is spatially constrained by the proximity of the nucleosome[47]. However, these investigations, performed in nuclear extracts, do not fully delineate the specific interplay between Polβ and its regulators like PARPs in the context of linker DNA. Furthermore, the entry/exit site of the nucleosome is associated with the linker histone H1, which promotes higher-order chromatin compaction and can further hinder the access of repair enzymes to DNA lesions[22,48]. Recent findings indicate that the dissociation of H1 from chromatin facilitates DNA repair, suggesting its dynamics is a key regulatory point[22,49].

In this study, we investigate the activity of Polβ on linker DNA and its functional interplay with the linker histone H1 and the PARP1/PARP2 system, including the HPF1 cofactor. We specifically focus on how an adjacent nucleosome core particle and its associated proteins modulate Polβ's choice between gap-filling and strand-displacement synthesis, a critical decision point in the BER sub-pathway selection.

Results

Stimulation of Polβ activity in Strand-Displacement Synthesis by an Adjacent Nucleosome Core Particle

Previous studies have consistently demonstrated that Polβ activity is substantially constrained within the nucleosome core, while its behavior on linker DNA adjacent to a nucleosome core particle (NCP) remains less explored. To investigate this aspect, we generated a nucleosome substrate with 50 bp and 30 bp linker arms, containing a 1-nt gap (gap-NCP227) located 26 bp from the 5' end of the longer linker (Fig. 1a). The nucleosome was reconstituted using the Widom 603 positioning sequence, which ensures a well-defined translational and rotational setting of the DNA.

Unexpectedly, we found that the efficiency of Polβ-catalyzed strand-displacement synthesis was higher on the gap-NCP227 substrate compared to the respective naked DNA (gap-DNA227). In identical reaction conditions, Polβ generated longer extension products when acting on gap-NCP (Fig. 1a). Kinetic experiments show more efficient strand-displacement synthesis on gap-NCP substrate at each time point (Fig. 1b). The initial rate of the single-nucleotide gap-filling reaction was also higher for gap-NCP than for gap-DNA: 24 fmol/s vs 12 fmol/s (Fig. 1c).

Considering the distributive nature of Polβ strand-displacement synthesis (typically incorporating 3 nucleotides per binding event), we propose several potential explanations for this phenomenon. First, the presence of NCP could influence the binding affinity of Polβ, potentially facilitating more rapid enzyme rebinding to the DNA template. Indeed, we observed a stepwise accumulation of DNA extension products with increasing length by increments of three nucleotides (e.g., +3, +6). This pattern is consistent with a model where the NCP enhances processivity by promoting enzyme rebinding. However, the binding affinity of Polβ was very similar for both gap-DNA227 and gap-NCP227, as detailed below.

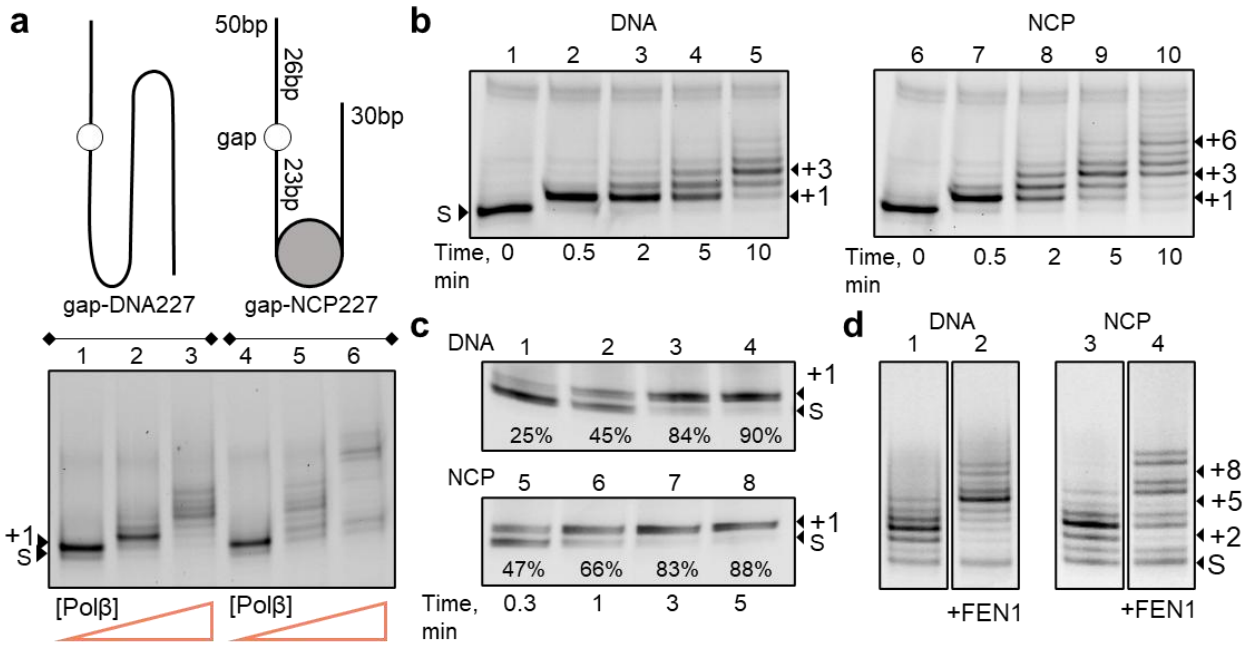

Fig. 1. Influence of downstream nucleosome on Polβ activity in linker DNA region. (a) Schematic structures of DNA and nucleosome, and electrophoregram showing DNA extension after incubation of gap-DNA or gap-NCP (50 nM) without or with Polβ (5 or 20 nM) and all four dNTPs (100 µM each) for 10 min. (b) Time-dependent extension of DNA upon incubation of 50 nM naked or nucleosomal gapped DNA (gap-DNA, lanes 1-5; gap-NCP, lanes 6-10) with Polβ (20 nM) and four dNTPs (100 µM each). (c) Time-dependent gap-filling reaction catalyzed by Polβ (4 nM) on gap-DNA or gap-NCP (50 nM) in the presence of dTTP (0.5 µM). The extent of substrate conversion is indicated at the bottom of the electropherograms. (d) Strand-displacement synthesis products generated by Polβ (25 nM) after incubation with gap-DNA (50 nM; lanes 1, 2) or gap-NCP (50 nM, lanes 3, 4) and four dNTPs (100 µM each), in the absence or presence of FEN1 (25 nM) for 5 min. Positions of substrate (S) and extension products (+n) in denaturing 20% PAG are indicated on the left and right of gel images.

Another factor that may influence the efficiency of strand-displacement synthesis is the interaction between the displaced single-stranded DNA flap (5'-flap) and the NCP. It is plausible that the flexible N-terminal tails of core histones could interact with the displaced flap, thereby facilitating destabilization and unwinding of DNA helix and enhancing the synthesis. Notably, the simple addition of free core histones to gap-DNA227 did not stimulate Polβ activity (Supplementary Fig. 1). On the contrary, free histones present at excessive relative to Polβ concentrations suppressed strand-displacement synthesis, likely due to competition with Polβ for the substrate binding via non-specific electrostatic interaction with the DNA.

To investigate interplay between the DNA strand-displacement synthesis and DNA flap cleavage, we analyzed the Polβ polymerase activity in the presence of flap endonuclease 1 (FEN1). Consistent with previous reports [7], the addition of FEN1 stimulated overall DNA synthesis by Polβ on both naked gap-DNA227 and gap-NCP227 substrate, as evidenced by an increased yield of long extension products (Fig. 1d). This is attributed to FEN1 resolving inhibitory secondary structures in the displaced flap, allowing Polβ to perform more processive synthesis. Strikingly, a particular pattern of products emerged specifically on the nucleosome substrate. The electrophoretic profile revealed a pronounced attenuation of bands corresponding to the incorporation of every third nucleotide (+2, +5, +8), creating a periodic pattern (Fig. 1d, lane 4). In contrast, the product distribution detected for the naked DNA was more uniform, without the pronounced periodic intensity pattern (Fig. 1d, lane 2). This observation suggests that exactly in the nucleosome, the cleavage of the displaced flap by FEN1 is exceptionally efficient and tightly coupled to

169 the synthetic cycle of Polβ. We hypothesize that upon the formation of a 3-nt flap – a preferred substrate
170 for FEN1 in the presence of NCP – the endonuclease immediately cleaves it, effectively "resetting" the
171 substrate and allowing Polβ to rapidly initiate the next synthetic cycle. This highly coordinated cycle results
172 in the observed rhythmic extension pattern, illustrating a processive "passing the baton" mechanism
173 uniquely facilitated by the nucleosome scaffold.
174
175 **Interaction of Polβ and its Possible Competitors with Gapped DNA and Nucleosome Substrates**
176 Next, we compared binding of Polβ with its nucleosome substrates using mass photometry (MP),
177 that measures the mass of individual biomolecules, allowing for the quantitative label-free analysis of
178 complex formation [50]. The theoretical mass of Polβ is 39 kDa, and of the nucleosome 248 kDa (108 kDa
179 histone octamer + 140 kDa DNA). At a 3:1 ratio of Polβ and gap-NCP227 concentrations, we detected a
180 complex with mass of 281±15 kDa (Fig 2a), indicating a 1:1 ratio of interaction (Polβ•gap-NCP227).
181 Complexes of 325, 371 and 414 kDa formed at increased gap-NCP227:Polβ ratio contained two, three and
182 four protein molecules. The calculated theoretical masses of these complexes are presented in Fig. 2b.

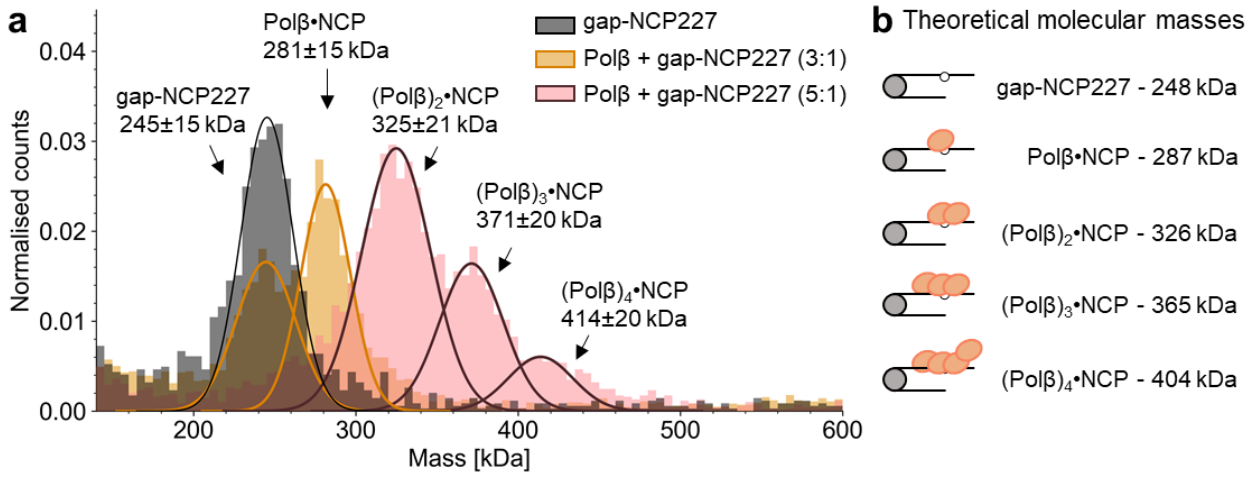

183
184 **Fig. 2.** Formation of Polβ complexes with gapped NCP substrate. (a) Mass photometry data: molecular
185 mass distribution of species in samples containing gap-NCP227 (5 nM) or its mixtures with Polβ (15 or 25
186 nM). (b) Calculated molecular masses of gap-NCP227 and its Polβ-associated complexes of different
187 stoichiometries.
188
189 Additional EMSA experiments indicated formation of higher-order complexes of Polβ with gap-
190 DNA227 and gap-NCP227, confirming the results of the MP assay (Supplementary Fig. 2a). Importantly,
191 we observed no oligomeric complexes of Polβ with non-gapped DNA227 or NCP227 substrates in either
192 EMSA or mass photometry experiments (Supplementary Fig. 2a, b)., indicating that the cooperative
193 binding is characteristic for Polβ interaction with its specific gapped substrate.
194 Then, we compared binding affinities of Polβ and its possible competitors (linker histone H1,
195 PARP1 and PARP2) for gap-DNA227, gap-NCP227, and nick-NCP227 (the product of 1-nt gap-filling
196 synthesis), using fluorescence titration assay to evaluate EC_{50} values (Table 1, Supplementary Fig. 2, c-f).
197

Table 1. EC_{50} values (nM) for protein complexes with DNA and nucleosomes

Substrate	PARP1	PARP2	H1	Polβ
gap-DNA	3 ± 0.3	3 ± 0.4	12 ± 2	1.5 ± 0.3
gap-NCP	3 ± 0.4	2 ± 0.3	8 ± 1	1 ± 0.2
nick-NCP	4 ± 0.6	1 ± 0.2	8 ± 1	2 ± 0.4

Statistically significant differences between EC_{50} values were evaluated by Student *t*-test; respective *p* values are presented in the text.

198

As shown in Table 1, the linker histone H1 exhibits the lowest affinity for DNA and nucleosomes, though its affinity for the NCP was 1.5-fold higher than for the naked DNA ($p \leq 0.05$), consistent with its specific binding at the nucleosome entry/exit site. PARP1 and PARP2 displayed comparable affinities for gap-DNA227 and gap-NCP227. However, PARP2 affinity for nick-NCP227 was higher than that of either PARP1 or Polβ ($p \leq 0.01$ and 0.05, respectively), aligning with previous reports [13,14]. As expected, Polβ exhibited higher affinity for the gapped substrates than for the single nucleotide insertion product (nick-NCP) ($p \leq 0.05$).

Linker Histone H1 Restricts Polβ Strand-Displacement Synthesis at the Nucleosome Entry/Exit Site

Linker histone H1 binds to linker DNA and facilitates chromatin compaction, which could potentially inhibit activities of DNA-dependent enzymes near the NCP boundary. We therefore analyzed the influence of H1 on Polβ-catalyzed strand-displacement synthesis. In our gap-NCP substrate, the incorporation of 24 nucleotides corresponds to synthesis within the linker DNA, and the subsequent synthesis proceeds into the nucleosomal DNA at superhelical locations (SHLs). While previous studies established severe constraints for strand-displacement synthesis within the NCP itself, here we detected the DNA synthesis initiating in the linker region and progressing into the nucleosome (Fig. 3a, lanes 1 and 3).

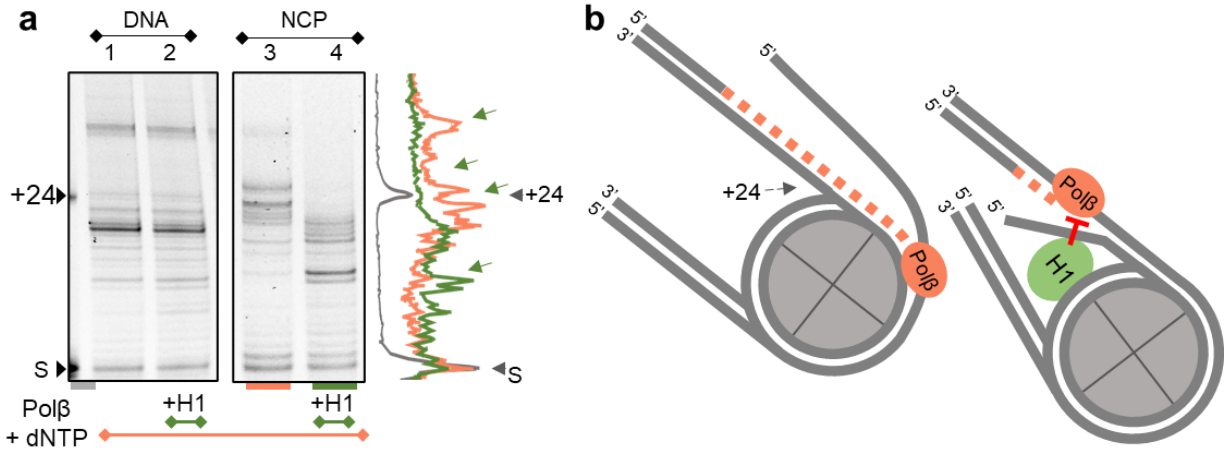

Fig. 3. Influence of linker histone H1 on Polβ activity. (a) Electrophoregrams show DNA extension by Polβ via strand-displacement synthesis after incubation of Polβ (50 nM) with four dNTPs (100 µM each), H1 (70 nM) and gap-DNA or gap-NCP (50 nM) for 10 min. Positions of the substrate and products of DNA synthesis in denaturing 20% PAG are indicated on the left and right of gel images. On the right are curves reflecting relative intensities of bands in samples compared (marked with color under the electropherogram). (b) Scheme shows proposed models of DNA extension by Polβ via strand-displacement synthesis on NCP or its complex with histone H1.

Under near single-turnover experimental conditions (i.e. at equimolar concentrations of Polβ and DNA substrate), we revealed no impact of H1 on Polβ activity on the naked DNA (Fig. 3a, lanes 1, 2). This result can be explained by non-specific binding of H1 to the naked DNA away from the gap site, occupied by Polβ due to its higher affinity for the gapped DNA/NCP (Table 1). In contrast, H1 significantly restricted the length of strand-displacement products synthesized near the nucleosome entry/exit site (Fig. 3a, lanes 3, 4), leading to accumulation of shorter extension products. Our data demonstrate that Polβ strand-displacement activity can be regulated not only by the nucleosome core but by the linker histone H1 also.

PARP1 and PARP2 Distinctly Modulate Polβ Activity on Nucleosomal Substrates

We further explored PARP1/PARP2 induced modulation of strand-displacement synthesis across a range of Polβ concentrations. The both PARPs reduced the yield of strand-displacement products (Fig.

4a, b). As expected, the extension by higher concentrations of Polβ was more effective in both the absence and presence of PARP1/PARP2. PARP1 appeared to suppress both 1-nt gap-filling and strand-displacement synthesis due to competition with Polβ for the gapped DNA/NCP substrate. PARP2 was similar to PARP1 in suppression of strand-displacement but less active in inhibiting the first nucleotide insertion, suggesting that PARP2 competes more strongly with Polβ for binding to the nicked DNA/NCP intermediate. Indeed, PARP2 has the highest affinity for nick-NCP227 compared to those of Polβ and PARP1 (Table 1). The difference between PARP1 and PARP2 in their inhibitory effects was further observed in experiments with fixed Polβ and increasing PARP concentrations. Even at a 10-fold excess over Polβ, PARP2 displayed no suppression of nicked intermediate production, in contrast to PARP1, which exhibited strong inhibition (Fig. 4c, d; Supplementary Fig. 3a). PARP2-induced inhibition of the single-nucleotide gap-filling reaction (performed in the presence of dTTP only) could be detected at a lower Polβ concentration and a shorter reaction time, when the extent of substrate conversion was below 50% (Supplementary Fig. 3b). Thus, competition between PARP2 and Polβ for interaction with the 1-nt DNA gap strongly depends on the experimental conditions.

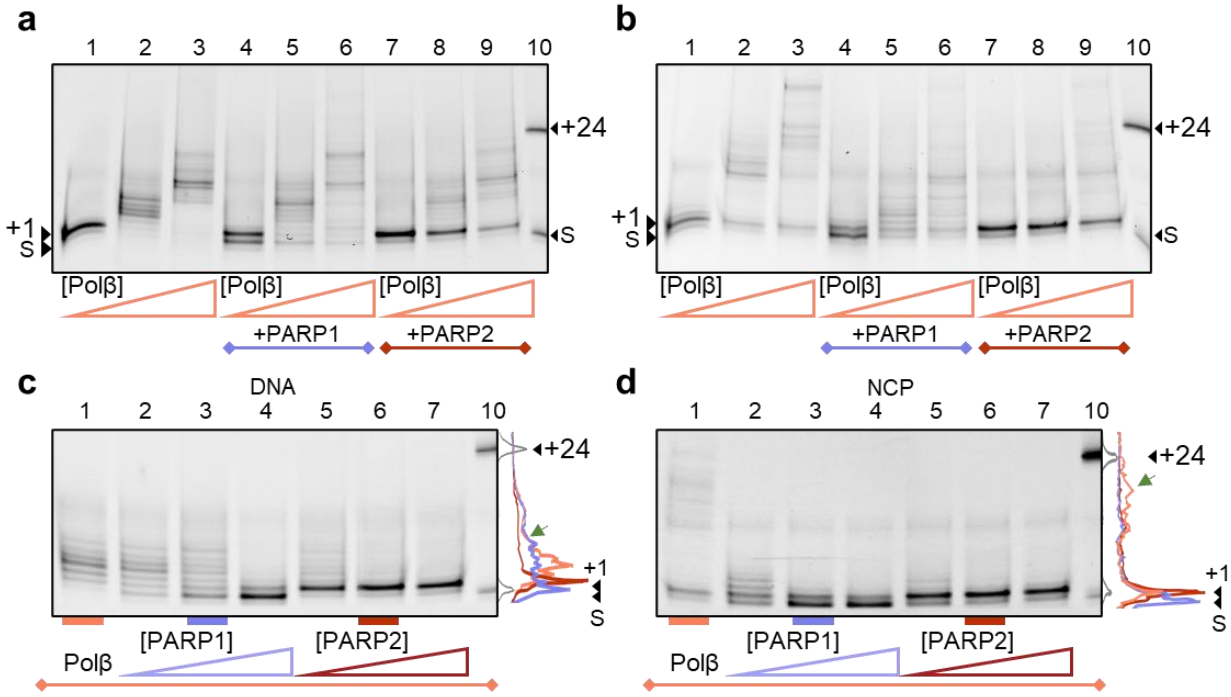

Fig. 4. Comparison of PARP1 and PARP2-induced effects on Polβ activity. a, b - Electrophoregrams show DNA extension by Polβ via strand-displacement synthesis after incubation of Polβ (3, 20 or 50 nM) with four dNTPs (100 μM each), PARP1/PARP2 (100 nM) and gap-DNA/gap-NCP (50 nM) for 10 min. c, d - DNA extension by Polβ via strand-displacement synthesis after incubation of Polβ (20 nM) with four dNTPs (100 μM each), PARP1/PARP2 (50, 100 or 200 nM) and gap-DNA/gap-NCP (50 nM). On the right are curves reflecting relative intensities of bands in samples compared (marked with color under the electropherogram). Positions of substrate and products of DNA synthesis in denaturing 20% PAG are indicated on the right of gel images.

Interestingly, the inhibition effects of both PARP1 and PARP2 were more pronounced on the nucleosome substrate than on the naked DNA. The maximum length of product synthesized in the presence of each PARP was always greater on the DNA than on the NCP at identical Polβ concentrations (Fig. 4a, b). Similarly, lower PARP1 and PARP2 concentrations were required to suppress synthesis on the NCP. Although no substantial difference in the binding affinity of Polβ, PARP1, or PARP2 for gap-DNA versus gap-NCP was detected (Table 1), it is evident that the proximal nucleosome modulates the functional interplay between PARP enzymes and Polβ at the DNA lesion.

PARylation Antagonizes the Inhibitory Action of PARPs and H1 on Strand-Displacement Synthesis

In the presence of NAD^+, PARP1 and PARP2 catalyze poly(ADP-ribose) (PAR) synthesis and transfer to target proteins, including automodification. AutoPARylation promotes the dissociation of PARPs from damaged DNA. Furthermore, these enzymes can PARylate core and linker histones in the presence of HPF1. We analyzed how addition of NAD^+ modulates the effects of PARP1 and PARP2 on Polβ-catalyzed DNA synthesis on the nucleosome, including in the presence of H1 and HPF1. As expected, the inhibitory action of PARP1 and PARP2 was nearly completely abolished in the presence of NAD^+; the efficiency of strand-displacement synthesis was restored under PARylation conditions (Fig. 5a, b; compare lanes 1 and 6). PARP1 suppressed the DNA synthesis most efficiently, compared to PARP2 and especially to H1, and this effect predominated when PARP1 and H1 were present together (Fig. 5a, compare lanes 3, 4 and 5). However, effects produced by PARP2 and histone H1 present together were different from those detected for each protein alone (Fig. 5b, compare lane 5 with lanes 3 and 4), indicating combined action of the both proteins. Most intriguingly, the restrictive effect on the length of extension products produced by H1 was not observed in PARylation conditions (Fig. 5a, b; compare lane 4 with lane 7). This fact was also observed in the presence of HPF1 (Supplementary Fig. 4). Additional experiments show that the inhibitory action of PARP1/PARP2 and H1 in PARylation conditions depends on the NAD^+ concentration known to control the efficiency of PAR elongation (Supplementary Fig. 5). These results suggest that the activity of PARP1 and PARP2 is sufficient to displace H1 from the nucleosome entry/exit site. This displacement could occur either through direct PARylation of H1 or via its non-covalent interaction with PAR[51]. To clarify the mechanism, we further analyzed the PARP1/PARP2 catalyzed modification of H1.

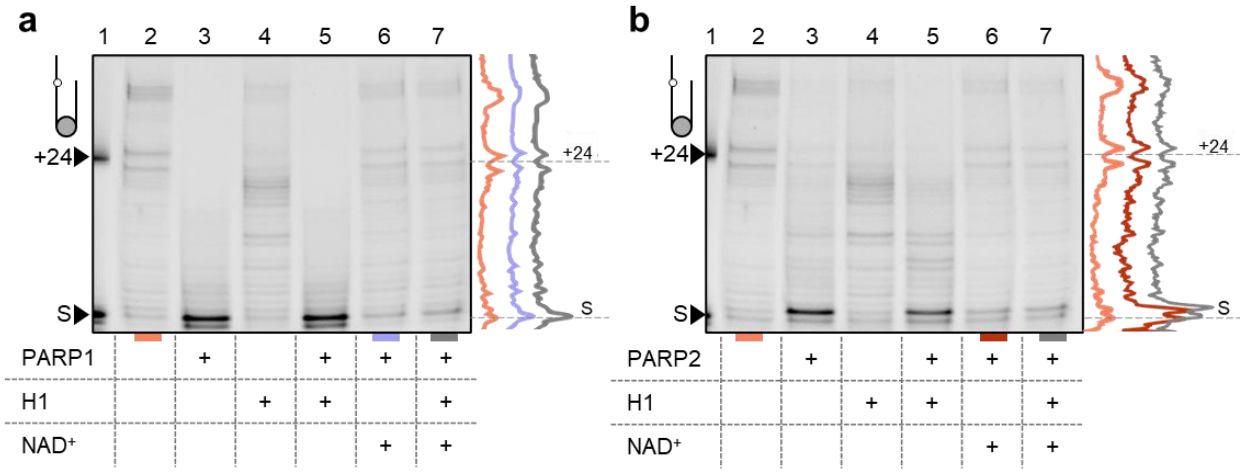

Fig. 5. Influence of H1 and PARylation on Polβ activity. (a, b) Electrophoregrams show DNA extension by Polβ via strand-displacement synthesis after incubation of Polβ (50 nM) with four dNTPs (100 µM each), H1 (75 nM), PARP1/PARP2 (100 nM), NAD^+ (10 µM) and gap-NCP (50 nM). PARylation was carried out by preliminary incubation of NCP mixtures with PARP1/PARP2 and NAD^+, with or without H1, for 30 min; further incubation with Polβ was performed for 10 min. Positions of substrate and products of DNA synthesis in denaturing 20% PAG are indicated on the left of gel images. On the right are curves reflecting relative intensities of bands in samples compared (marked with color under the electropherogram).

Linker histone H1 is modified by PARP1 and PARP2 in a HPF1-dependent manner

The PARylation-dependent action of histone H1 on Polβ activity prompted us to explore the direct PARylation of H1. The PARylation reaction was performed using gap-NCP for PARP1/PARP2 activation in the presence and absence of HPF1 (Fig. 6). PARP1 was more active in the automodification than in histone modification, whereas PARP2 catalyzed more efficiently ADP-ribosylation of histones (Fig. 6a, c), consistent with our previous studies [16,17,43]. The presence of H1 reduced the level of HPF1-dependent modification of core histones by the both enzymes due to redistribution of PARylation targets between the linker and core histones (Fig. 6a, c; compare samples 4, 8 with samples 2, 7). In the absence of HPF1,

305 modification of H1 was detected only at its increased concentration as evidenced from analysis of ADP-
306 ribosylation products after treatment of reaction mixtures with poly(ADP-ribose) glycohydrolase (PARG)
307 (Fig. 6b, d, e and Supplementary Fig. 6). Thus, the very low level of HPF1-independent PARylation of H1
308 by PARP1/PARP2 is most likely insufficient to induce the linker histone dissociation. Additional
309 fluorescence anisotropy experiments showed that while H1 slowed down the dissociation kinetics of
310 PARP1/PARP2 from the complex with gap-NCP, it did not affect the final level of anisotropy
311 (Supplementary Fig. 7)., suggesting that H1 dissociates from the complex together with PARPs under
312 PARylation conditions. Therefore, the eviction of H1 is mediated rather by its high-affinity interaction with
313 PAR (demonstrated previously [51,52]) than by direct PARylation (which is minimal without HPF1). We
314 propose that automodification of PARP1 and PARP2 leads to the recruitment of H1 away from the
315 nucleosome via attraction to PAR, ultimately permitting strand-displacement synthesis to proceed
316 through the nucleosome entry/exit region.

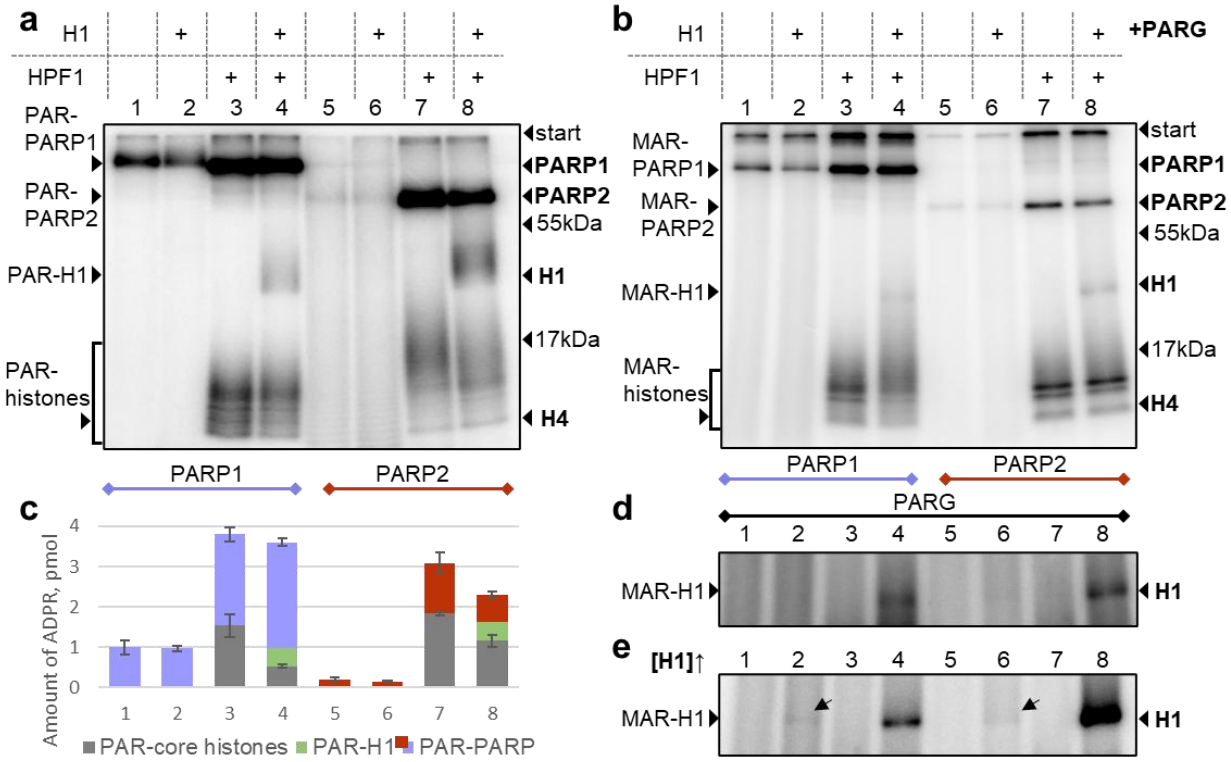

317
318 **Fig. 6.** PARylation of histone H1 depends on HPF1. a, b - Autoradiograms show covalent binding of ^{32}P-
319 labelled PAR or MAR to protein targets after incubation of PARP1/PARP2 (500 nM) with [^{32}P]NAD$^+$ (1 µM),
320 H1 (70 nM), HPF1 (1 µM) and gap-NCP (250 nM) for 30 min, before (a) and after (b) subsequent treatment
321 of reaction mixtures with PARG. Positions of ADP-ribosylated proteins and their native forms (and
322 molecular weight markers) in 20% SDS-PAG are indicated on the left and right of gel images. c - Histograms
323 show the amount of PAR attached to PARP1/PARP2, H1 and histones in the distinct samples (the mean ±
324 SD, n=3). d, e - Autoradiograms show covalent binding of ^{32}P-labelled MAR to H1 after incubation of
325 PARP1/PARP2 (500 nM) with [^{32}P]NAD$^+$ (1 µM), H1 (d, 300 nM; e, 500 nM), HPF1 (1 µM) and gap-NCP (250
326 nM) for 45 min,, and following PARG treatment. Positions of mono-ADP-ribosylated H1 and its native form
327 in 20% SDS-PAG are indicated on the left and right of gel images.
328
329 Interestingly, the yields of PARylated core histones and their lengths were quite different in the
330 absence and presence of H1, but the yields of MARylated products were practically independent on the
331 presence of H1 (compare lanes 2, 4, 7 and 8 in Fig. 6a with respective lanes in Fig. 6b). These data suggest
332 that H1 inhibits primarily modification of core histones at the elongation stage. This could be related to

333 different stabilities of complexes formed by the linker histone and core histones with DNA or speaks in
334 favor of H1 interaction with PAR, which may influence the PAR length[53].
335
336 **Discussion**
337 The canonical view of chromatin as a passive barrier to DNA repair has been increasingly refined
338 to encompass its role as an active regulator of repair pathway choice[19,28,47]. While it is well established
339 that the nucleosome core particle (NCP) profoundly suppresses the activity of BER enzymes, most studies
340 have focused on lesions buried within the nucleosomal DNA and the regulatory landscape of the linker
341 DNA has remained less explored[47]. While a lesion within the core DNA is subject to severe steric
342 hindrance[14,21–24,38], a lesion in the linker is physically accessible yet its processing is influenced by the
343 nearby NCP. Here, we investigate DNA repair synthesis in the linker DNA and reveal how the adjacent
344 NCP, in conjunction with associated proteins, creates a unique regulatory environment that modulates
345 the activity of Polβ and its decision between short-patch (SP) and long-patch (LP) sub-pathways of BER.
346 Our most striking finding is that NCP can stimulate Polβ-catalyzed single-nucleotide gap-filling and
347 strand-displacement synthesis on adjacent linker DNA, instead of expected suppression. We propose that
348 the NCP may act as a "steric anchor" promoting the rapid rebinding of Polβ to its DNA substrate, thereby
349 effectively increasing its local concentration and processivity. Considering the distributive nature of DNA
350 synthesis catalyzed by Polβ, such facilitated rebinding would lead to an increased rate of DNA synthesis
351 and a greater number of nucleotides incorporated, which is precisely what we observe in the presence of
352 the nucleosome. This stimulatory effect extends beyond Polβ alone. Our data reveal that the presence of
353 an adjacent nucleosome not only influences Polβ activity but also orchestrates its functional interplay with
354 downstream enzyme of the LP BER pathway, FEN1. The rhythmic pattern of extension products, where
355 bands corresponding to every third nucleotide are faint, detected specifically on the nucleosome
356 substrate, is highly indicative of effective substrate channeling, probably via "passing the baton"
357 mechanism [5]. Consistent with this model, the interaction of PARP1, Polβ and FEN-1 at the branch-point
358 BER intermediate has been directly demonstrated by their co-precipitation following photocrosslinking to
359 this DNA intermediate in cell extracts[54]. Importantly, this coordination on the nucleosome contrasts with
360 the more stochastic and asynchronous product distribution on naked DNA, indicating that the nucleosome
361 context actively facilitates efficient handoff between repair enzymes. In addition, the inhibitory effects of
362 both PARP1 and PARP2 (discussed below) were more pronounced on the nucleosome substrate than on
363 the naked DNA, despite similar binding affinities. It has been shown previously that the protein assembly
364 for the specific repair process can be coordinated by protein-protein interactions which were determined
365 for the core enzymes of BER[54–57]. Here we propose that the nucleosome itself functions as an allosteric
366 platform that modulates the assembly, activity and regulation of the BER machinery and fosters a
367 coordinated substrate channeling. This hypothesis is supported by recent structural work revealed specific
368 mechanisms of nucleosome binding by DNA repair enzymes[58,59].
369 Furthermore, we demonstrate that Polβ forms high-order complexes on gapped DNA and
370 nucleosome substrates via multimerization. This propensity for self-association has been previously noted
371 for many BER players, including PARP1 and PARP2[17,55,60] and for Polβ on gapped and template-primer
372 structures[61]. This observation raises the possibility that multiple cycles of Polβ binding and flap
373 endonuclease-catalyzed cleavage could be coordinated through such multimeric assemblies.
374 The stimulatory effect of nucleosome is balanced by the suppressive action of linker histone H1,
375 which in turn is controlled by PARP-catalyzed PAR synthesis. The linker histone H1 contributing to
376 chromatin compaction[62–64] limits Polβ-catalyzed DNA repair synthesis at the entry/exit site of nucleosome.
377 Critically, this restriction is reversed by PARP1/PARP2-catalyzed PARylation. While eviction of histone H1
378 *in vivo* and its function as a high-affinity PAR-reader in vitro have been established[49,51,52,65,66], the dominant
379 mechanism of H1 PARylation-dependent function remains unclear[67]. Our data show that H1 displacement
380 from DNA occurs even when its direct PARylation (detected in the absence of HPF1) is minimal, favoring
381 a model where H1 is sequestered via PAR-mediated interaction with automodified PARP (Fig. 7). This

382 provides a dynamic, PARylation-controlled mechanism for primary chromatin relaxation required for DNA
383 repair.
384 Our findings refine the distinct roles of PARP1 and PARP2 in BER. The both PARPs are well
385 established to suppress strand-displacement synthesis via competition with BER enzymes for DNA
386 intermediates[12,13,38,54,68]. The distinct binding preferences of PARP1 and PARP2 for the BER DNA
387 intermediates[13,14,17], coupled with their stage-specific inhibitory effects, suggest a functional
388 specialization: PARP1 appears to modulate predominantly the initial stages of BER, while PARP2 exerts a
389 major impact on the following steps (DNA synthesis and ligation). In our experiments, both enzymes
390 compete with Polβ for substrate binding, but their modes of inhibition are distinct. PARP1 suppresses 1-
391 nt gap-filling and strand-displacement synthesis, consistent with its high affinity for the initial gapped
392 intermediate. In contrast, PARP2, with its pronounced preference for the nicked DNA, specifically and
393 potently inhibits the strand-displacement and is less effective at the stage of the first nucleotide insertion.
394 Thus, the DNA synthesis step itself demarcates the functional boundary between the regulatory spheres
395 of PARP1 and PARP2 within the BER pathway. This positions PARP2 as a dedicated «game changer» of the
396 SP/LP BER decision point. By "capping" the nick after gap-filling, PARP2 prevents strand-displacement,
397 biasing repair towards the short-patch pathway – a critical function in linker DNA, which lacks the inherent
398 physical constraints of the nucleosome core. Importantly, this role of PARP2 in binding and protecting
399 nicked DNA intermediates provides a mechanistic basis for its reported involvement in PARP inhibitor
400 cytotoxicity. It has been proposed that PARP2, trapped on nicks associated with Okazaki fragments during
401 DNA replication, prevents their ligation, leading to cell death[69–71].

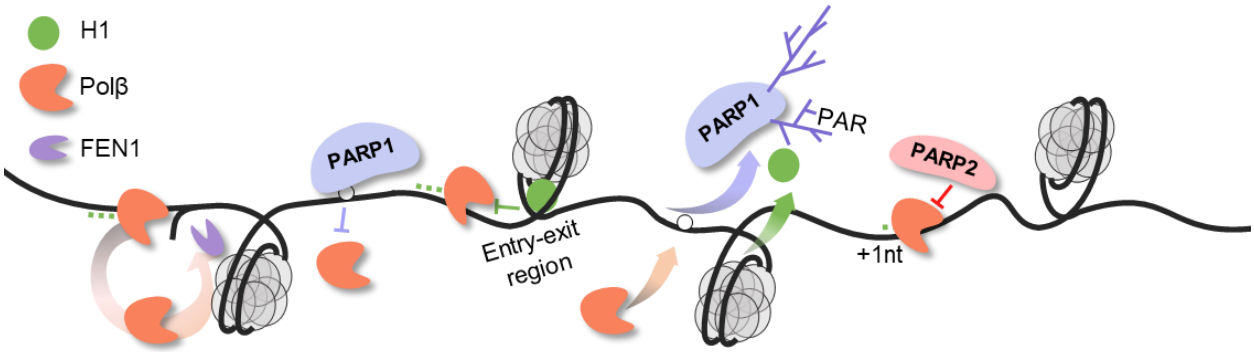

402
403 **Fig. 7.** A model of multi-layered regulation of Polβ activity in a nucleosomal context. The nucleosome core
404 particle acts as a platform that facilitates the coordinated action of BER enzymes at a proximal damage
405 site in linker region. Linker histone H1 and PARP1 suppress DNA synthesis; however, activation and
406 autoPARylation of PARP1 at the lesion alleviates this restriction. PARP2, by inhibiting strand-displacement
407 synthesis, serves as a molecular switch from long-patch (LP) to short-patch (SP) BER.
408
409 Thus, our study elucidates a multi-layered system to regulate Polβ activity at the crucial interface
410 between the nucleosome core and the linker DNA. The different affinities of PARP1 and PARP2 for distinct
411 BER intermediates create a regulatory cascade to choose between short- and long-patch repair. The
412 nucleosome may act as an active participant that influences the organization of repair factors, their
413 kinetics, and the processing of DNA damage.
414
415 **Materials and methods**
416 Recombinant wild-type human PARP1 and murine PARP2 were purified as described previously[72].
417 Recombinant wild-type human HPF1 and H1.0 were purified as described previously [43]. Human APE1,
418 FEN1 and rat Polβ were purified as described previously[73–76]. All proteins were tested for DNA polymerase
419 activity (Supplementary Fig. 8a). *E. coli* uracil-DNA glycosylase (UDG) and *T. aquticus* DNA polymerase
420 were from Biosan (Novosibirsk, Russia). Core histones were isolated from *Gallus gallus* erythrocytes and
421 purified as described previously [77]. pGEM-3z/603 was a gift from J. Widom (Addgene plasmid #26658;

422 http://n2t.net/addgene:26658; RRID: Addgene_26658). Synthetic oligodeoxyribonucleotides were
423 purchased from Genterra (Moscow, Russia). The ^{32}P-labelled NAD^+ was synthesized enzymatically as
424 described previously[78], using [α-^{32}P]ATP (with specific activity of 3000 Ci/mmol, synthesized in the
425 Laboratory of Biotechnology, ICBFM, Novosibirsk, Russia). NAD^+ and reagents for electrophoresis and
426 basic components of buffers were purchased from Sigma–Aldrich (USA). Double-distilled water was used
427 to prepare all buffer solutions and reaction samples. Sequences of the oligonucleotides are presented
428 in Table 2.
429

Table 2. Sequences of synthetic oligonucleotides used in the study.	
Primers for 227 bp DNA	Upstream: 5'-CCTCTAGAGTCGGGAGC[**dT-FAM**]CGGAACAC[**dU**]ATCCGACTGGC-3' Downstream: 5'-GAGCCGTAAAATAATCGACACTCTCGGGTGCCCAGTTCG-3'
Controls for gel mobility	5'-CCTCTAGAGTCGGGAGC[**dT-FAM**]CGGAACAC-3' 5'-CCTCTAGAGTCGGGAGC[**dT-FAM**]CGGAACACTATCCGACTGGCACCGAAACGGGT-3'

430
431 **Methods**
432 **Preparation of DNA and nucleosomes**
433 Model 227 bp DNA containing the 147-bp core of the 603 nucleosome positioning sequence [79] was
434 generated by PCR from the pGEM-3z/603 plasmid using the oligonucleotide primers (Table 2).
435 Nucleosomes were assembled by mixing DNA and core histones in a high-salted buffer containing 2 M
436 NaCl, dialyzed against the NaCl concentration gradient from 2 M to 65 mM during 6 h at 4 °C and then
437 against the buffer with 10 mM NaCl overnight at 4 °C with gentle stirring. The optimal ratios of DNA and
438 histones were determined in preliminary quick-time experiment as described in the published protocol[77].
439 The homogeneity of the DNA and NCP samples was analyzed by the EMSA on a 4% nondenaturing PAG
440 (Supplementary Fig. 8b).
441 To generate a single-nucleotide gap in DNA substrates, reaction mixtures containing 1 µM DNA or
442 NCP, uracil-DNA glycosylase (UDG, 1 activity unit per 0.6 pmol of DNA/NCP), and 0.1 µM AP endonuclease
443 1 (APE1) in reaction buffer (50 mM Tris-HCl (pH 8.0), 50 mM NaCl, 5 mM $MgCl_2$, 1 mM DTT) were incubated
444 for 30 min at 37 °C. To obtain nicked NCP (nick-NCP) substrate, reaction mixtures containing 166 nM gap-
445 NCP, 16.6 nM Polβ and 10 µM dTTP in the reaction buffer were incubated for 10 min at 37 °C. Then the
446 mixture was diluted with buffer (50 mM Tris-HCl (pH 8.0), 50 mM NaCl, 10 mM EDTA, 1 mM DTT) to 6 nM
447 concentration of NCP and incubated for 10 min at 45°C. The homogeneity of nick-NCP was analyzed by
448 EMSA on a 4% nondenaturing PAG (Supplementary Fig. 8b).
449
450 **Fluorescence studies of Polβ/H1/PARP1/PARP2 interaction with DNAs/NCPs**
451 The affinity of proteins for DNA and NCP substrates was evaluated by determining the half-maximal
452 effective concentration (EC_{50}) of protein complexes with FAM-labeled DNA or NCP using fluorescence
453 anisotropy measurements [80]. Briefly, reaction mixtures containing 0–400 nM PARP1/PARP2/H1/Polβ and
454 3 nM of gap-DNA (227 bp), gap-NCP, or nick-NCP in binding buffer (50 mM Tris-HCl pH 8.0, 50 mM NaCl,
455 10 mM EDTA, 1 mM DTT) were prepared on ice in a 384-well plate and incubated for 5 min at room
456 temperature. Fluorescence anisotropy measurements were performed using a CLARIOstar microplate
457 reader (BMG Labtech). Fluorescent probes were excited at 495 nm, and emission was detected at 520 nm.
458 Each measurement consisted of 50 flashes per well, and fluorescence intensity values were averaged
459 automatically. Measurements for each well were performed three times at 1-min intervals. The averaged
460 values were used for final plotting, and EC_{50} values were calculated using the SMART Control Data Analysis
461 software (BMG LABTECH). The data were plotted (F vs C) and fitted to four-parameter logistic equation: F
462 $= F_0 + (F_\infty - F_0)/[1 + (EC_{50}/C)^n]$, where F is the measured fluorescence anisotropy of a solution containing
463 the labeled DNA at a given concentration (C) of proteins, F_0 is the fluorescence anisotropy of solution of

464 the labeled DNA alone, F_∞ is the fluorescence anisotropy of the labeled DNA saturated with the protein,
465 EC_{50} is the concentration of the protein at which $F - F_0 = (F_\infty - F_0)/2$, and n is the Hill coefficient, which
466 denotes the steepness (slope) of the nonlinear curve.
467
468 **Mass Photometry measurements of Polβ interaction with gap-NCP**
469 The stoichiometry of Polβ complexes with gap-NCP was assessed by mass photometry using a
470 TwoMP mass photometer (Refeyn, UK). Briefly, 10 µl buffer (50 mM Tris-HCl (pH 8,0), 50 mM NaCl, 5 mM
471 $MgCl_2$, 1 mM DTT) was loaded to the sample chamber and the objective was focused by autofocus
472 function. Then 0.5 µl sample containing 60 nM gap-NCP alone or together with 180 nM or 200 nM Polβ
473 was added to the chamber and mixed by pipetting. The buffer was preliminary ultrafiltered by using
474 Sartorius vivaspin columns with 1000 kDa pore PES membrane filter. The reaction mixture was prepared
475 on ice and incubated for 5 min at room temperature. Data were collected for 1 min using the AcquireMP
476 software (Refeyn, UK). All samples were measured using the expanded detection area. The mass
477 photometry signals were calibrated using BSA (69 kDa) (Sigma-Aldrich, USA), recombinant PARP1 protein
478 (113 kDa) and recombinant Cas9 protein (158 kDa). Mass photometry data were analyzed using the
479 DiscoverMP software (Refeyn, UK) to calculate relative molecular populations from the areas of the
480 Gaussian peaks (representing free NCP and its complexes with one or several Polβ molecules).
481
482 **Testing of Polβ-catalyzed DNA synthesis**
483 DNA synthesis catalyzed by Polβ was performed in 5 µL reaction mixtures containing 50 nM gap-
484 DNA (227 bp) or gap-NCP, 20 nM Polβ (unless stated otherwise), and either 100 µM of each of four dNTPs
485 (for strand-displacement synthesis) or 500 nM dTTP (for gap-filling synthesis) in reaction buffer (50 mM
486 Tris-HCl pH 8.0, 50 mM NaCl, 5 mM $MgCl_2$, 1 mM DTT). Polβ concentration was varied from 3 nM to 75
487 nM depending on the experiment. To analyze the influence of FEN1, H1, PARP1 or PARP2 on the Polβ DNA
488 polymerase activity mixtures were supplemented with 25 nM FEN1, 170 nM H1, 50–200 nM PAPR1 or
489 PARP2 respectively. To analyze the influence of H1 and PARylation on Polβ activity, mixtures (the final
490 volume was 10 µl) of 50 nM gap-DNA or gap-NCP, 100 nM PAPR1 or PARP2, 75 nM H1, and 10 µM NAD^+
491 in reaction buffer (50 mM Tris-HCl (pH 8.0), 150 mM NaCl, 5 mM $MgCl_2$, 1 mM DTT) were incubated at
492 37°C for 30 min for the PARylation reaction. After this, Polβ and dNTPs were added to the mixtures to
493 final concentrations of 20 nM Polβ and 100 µM of each dNTP. After adding of Polβ and dNTPs, the mixtures
494 were incubated at 37 °C for 10 min.
495 All reactions were terminated by adding 10 µL of 8 M urea with 20 mM EDTA, followed by heating
496 at 80 °C for 10 min and 97 °C for 1 min. Reaction products were separated by electrophoresis on 20%
497 denaturing polyacrylamide gels. FAM-labeled oligonucleotides of 26 nt and 50 nt length (Table 2) were
498 used as gel-mobility controls corresponding to the length of substrate and linker. Gels were visualized
499 using a Typhoon FLA 9500 scanner (GE Healthcare Life Sciences, USA). The relative intensities of bands
500 corresponding to the substrate and products were quantified using Quantity One 4.6.6 software (Bio-Rad,
501 USA).
502
503 **Kinetic measurements of Polβ activity**
504 The reaction of DNA synthesis via strand displacement catalyzed by Polβ was carried out in a 70
505 µl reaction mixture containing 50 mM Tris-HCl, pH 8.0, 50 mM NaCl, 5 mM $MgCl_2$, 50 nM gap-DNA (227
506 bp) or gap-NCP, 20 nM Polβ and 100 µM each of four dNTPs. Reactions were initiated by addition of dNTPs
507 and stopped after 30 s, 2 min, 5 min and 10 min of incubation by adding 5 µl aliquot of the reaction mixture
508 to 5 µl of 8 M urea with 20 mM EDTA. For kinetic analysis of gap-filling synthesis, the reaction mixture
509 contained 50 mM Tris-HCl, pH 8.0, 50 mM NaCl, 5 mM $MgCl_2$, 200 nM gap-DNA/gap-NCP, 4 nM Polβ and
510 500 nM dTTP. Reactions were initiated by addition of dTTP and stopped after 20 s, 1 min, 3 min and 5 min
511 of incubation. Reaction products were separated and analyzed as described in subsection above.
512

513 **Protein PARylation reaction**

514 Reaction mixtures containing 125 nM gap-NCP, 250 nM PARP1 or PARP2, 500 nM HPF1, 150 nM
515 H1, and 1 µM [^{32}P]NAD^{+} in buffer (50 mM Tris-HCl pH 8.0, 50 mM NaCl, 5 mM $MgCl_2$, 1 mM DTT) were
516 incubated for 30 min at 37 °C. Reactions were stopped by adding 1.2 µL of inhibitor solution (50 µM
517 olaparib, 100 mM EDTA, 25 mM Tris-HCl pH 8.0, 25 mM NaCl, 500 µM DTT). When indicated, 1 µM PARG
518 was added to the mixtures, followed by incubation for 1 h at 37 °C to digest PAR. Subsequently, 1.5 µL of
519 SDS-PAGE sample buffer was added, and samples were heated at 97 °C for 5 min. Reaction products were
520 separated by 20% SDS-PAGE, visualized by phosphorimaging, and quantified using a Typhoon imaging
521 system (GE Healthcare Life Sciences) and Quantity One Basic software (Bio-Rad).
522

523 **Acknowledgements**

524 We would like to thank the entire laboratory of bioorganic chemistry of enzymes for feedback. We
525 acknowledge Svetlana N. Khodyreva for preparation of recombinant FEN1, Anton V. Endutkin and Dmitry
526 O. Zharkov for supporting Mass Photometry experiments. The reported study was funded by the Russian
527 state-funded project for ICBFM SB RAS № 125012300658-9 (use of shared equipment for experimental
528 work, MP experiments) and by the Russian Science Foundation № 25-74-10025 (preparation of proteins
529 and nucleosomes) and 25-74-30006 (biochemical experiments).
530

531 **Author information**

532 Affiliations
533 Institute of Chemical Biology and Fundamental Medicine, SB RAS, Novosibirsk, Russia
534 Shtanov D.M., Kurgina, T. A., Kutuzov, M. M., Naumenko, K. N., Ukraintsev A. A., Moor, N. A., Lavrik, O. I.
535

536 **Contributions**

537 D.M.S. performed the experiments, T.A.K. performed the experiments and created the figures. M.M.K.,
538 K.N.N., A.A.U. and N.A.M. contributed to the study with protein purification and nucleosome assembling.
539 T.A.K., N.A.M. and O.I.L. analyzed the data and wrote the manuscript. All authors reviewed the results and
540 approved the final version of the manuscript.

541 Corresponding author
542 Correspondence to Olga I. Lavrik
543

544 **Competing interests**

545 The authors declare no competing interests.
546

547 **Additional information**

548 **Supplementary information** The online version contains supplementary material available at

549 **References**

550 Fortini, P. *et al.* Different DNA polymerases are involved in the short- and long-patch base excision
551 repair in mammalian cells. *Biochemistry* **37**, 3575–3580 (1998).
552 2. Beard, W. A. & Wilson, S. H. Structure and mechanism of DNA polymerase β. *Biochemistry* **53**, 2768–
553 2780 (2014).
554 3. Sattler, U., Frit, P., Salles, B. & Calsou, P. Long-patch DNA repair synthesis during base excision
555 repair in mammalian cells. *EMBO Rep.* **4**, 363–367 (2003).
556 4. Singhal, R. K. & Wilson, S. H. Short gap-filling synthesis by DNA polymerase beta is processive. *J. Biol.*
557 *Chem.* **268**, 15906–15911 (1993).
558 5. Wilson, S. H. & Kunkel, T. A. Passing the baton in base excision repair. *Nat. Struct. Biol.* **7**, 176–178
559 (2000).
560 6. Prasad, R., Dianov, G. L., Bohr, V. A. & Wilson, S. H. FEN1 stimulation of DNA polymerase beta
561 mediates an excision step in mammalian long patch base excision repair. *J. Biol. Chem.* **275**, 4460–
562 4466 (2000).
563 7. Liu, Y. *et al.* DNA polymerase beta and flap endonuclease 1 enzymatic specificities sustain DNA
564 synthesis for long patch base excision repair. *J. Biol. Chem.* **280**, 3665–3674 (2005).
565 8. Chagovetz, A. M., Sweasy, J. B. & Preston, B. D. Increased activity and fidelity of DNA polymerase
566 beta on single-nucleotide gapped DNA. *J. Biol. Chem.* **272**, 27501–27504 (1997).
567 9. Canitrot, Y. *et al.* Nucleotide excision repair DNA synthesis by excess DNA polymerase beta: a
568 potential source of genetic instability in cancer cells. *FASEB J. Off. Publ. Fed. Am. Soc. Exp. Biol.* **14**,
569 1765–1774 (2000).
570 10. Fréchet, M., Canitrot, Y., Cazaux, C. & Hoffmann, J. S. DNA polymerase beta imbalance increases
571 apoptosis and mutagenesis induced by oxidative stress. *FEBS Lett.* **505**, 229–232 (2001).
572 11. Gibson, B. A. & Kraus, W. L. New insights into the molecular and cellular functions of poly(ADP-
573 ribose) and PARPs. *Nat. Rev. Mol. Cell Biol.* **13**, 411–424 (2012).
574 12. Sukhanova, M. V. Human base excision repair enzymes apurinic/apyrimidinic endonuclease1 (APE1),
575 DNA polymerase and poly(ADP-ribose) polymerase 1: interplay between strand-displacement DNA
576 synthesis and proofreading exonuclease activity. *Nucleic Acids Res.* **33**, 1222–1229 (2005).
577 13. Sukhanova, M. V. *et al.* A Single-Molecule Atomic Force Microscopy Study of PARP1 and PARP2
578 Recognition of Base Excision Repair DNA Intermediates. *J. Mol. Biol.* **431**, 2655–2673 (2019).
579 14. Kutuzov, M. M. *et al.* The contribution of PARP1, PARP2 and poly(ADP-ribosyl)ation to base excision
580 repair in the nucleosomal context. *Sci. Rep.* **11**, 4849 (2021).
581 15. Sukhanova, M., Khodyreva, S. & Lavrik, O. Poly(ADP-ribose) polymerase 1 regulates activity of DNA
582 polymerase β in long patch base excision repair. *Mutat. Res. - Fundam. Mol. Mech. Mutagen.* **685**,
583 80–89 (2010).
584 16. Kurgina, T. A., Moor, N. A., Kutuzov, M. M. & Lavrik, O. I. The HPF1-dependent histone PARylation
585 catalyzed by PARP2 is specifically stimulated by an incised AP site-containing BER DNA intermediate.
586 *DNA Repair* **120**, 103423 (2022).
587 17. Kurgina, T. A., Moor, N. A., Kutuzov, M. M., Endutkin, A. V. & Lavrik, O. I. Deciphering the dark side
588 of histone ADP-ribosylation: what structural features of damaged nucleosome regulate the activities
589 of PARP1 and PARP2. *Nucleic Acids Res.* **53**, gkaf864 (2025).
590 18. Khodyreva, S. N. *et al.* Apurinic/apyrimidinic (AP) site recognition by the 5'-dRP/AP lyase in
591 poly(ADP-ribose) polymerase-1 (PARP-1). *Proc. Natl. Acad. Sci. U. S. A.* **107**, 22090–22095 (2010).
592 19. Davey, C. A., Sargent, D. F., Luger, K., Maeder, A. W. & Richmond, T. J. Solvent mediated interactions
593 in the structure of the nucleosome core particle at 1.9 a resolution. *J. Mol. Biol.* **319**, 1097–1113
594 (2002).
595 20. Vito, A. F., Boesch, D. J., Hammons, A. M., Freudenthal, B. D. & Weaver, T. M. Base excision repair in
596 chromatin: A tug-of-war for DNA damage. *DNA Repair* **155**, 103908 (2025).

21. Nilsen, H., Lindahl, T. & Verreault, A. DNA base excision repair of uracil residues in reconstituted nucleosome core particles. *EMBO J.* **21**, 5943–5952 (2002).
22. Menoni, H., Shukla, M. S., Gerson, V., Dimitrov, S. & Angelov, D. Base excision repair of 8-oxoG in dinucleosomes. *Nucleic Acids Res.* **40**, 692–700 (2012).
23. Cannan, W. J., Rashid, I., Tomkinson, A. E., Wallace, S. S. & Pederson, D. S. The Human Ligase IIIα-XRCC1 Protein Complex Performs DNA Nick Repair after Transient Unwrapping of Nucleosomal DNA. *J. Biol. Chem.* **292**, 5227–5238 (2017).
24. Weaver, T. M. *et al.* Structural basis for APE1 processing DNA damage in the nucleosome. *Nat. Commun.* **13**, 5390 (2022).
25. Beard, B. C., Wilson, S. H. & Smerdon, M. J. Suppressed catalytic activity of base excision repair enzymes on rotationally positioned uracil in nucleosomes. *Proc. Natl. Acad. Sci. U. S. A.* **100**, 7465–7470 (2003).
26. Nakanishi, S., Prasad, R., Wilson, S. H. & Smerdon, M. Different structural states in oligonucleosomes are required for early versus late steps of base excision repair. *Nucleic Acids Res.* **35**, 4313–4321 (2007).
27. Hinz, J. M., Rodriguez, Y. & Smerdon, M. J. Rotational dynamics of DNA on the nucleosome surface markedly impact accessibility to a DNA repair enzyme. *Proc. Natl. Acad. Sci. U. S. A.* **107**, 4646–4651 (2010).
28. Rodriguez, Y. & Smerdon, M. J. The structural location of DNA lesions in nucleosome core particles determines accessibility by base excision repair enzymes. *J. Biol. Chem.* **288**, 13863–13875 (2013).
29. Weaver, T. M. *et al.* Structural basis of gap-filling DNA synthesis in the nucleosome by DNA Polymerase β. *Nat. Commun.* **16**, 2607 (2025).
30. Adar, S., Hu, J., Lieb, J. D. & Sancar, A. Genome-wide kinetics of DNA excision repair in relation to chromatin state and mutagenesis. *Proc. Natl. Acad. Sci. U. S. A.* **113**, E2124-2133 (2016).
31. Pich, O. *et al.* Somatic and Germline Mutation Periodicity Follow the Orientation of the DNA Minor Groove around Nucleosomes. *Cell* **175**, 1074-1087.e18 (2018).
32. Cordero, C. *et al.* Contributing factors to the oxidation-induced mutational landscape in human cells. *Nat. Commun.* **15**, 10722 (2024).
33. Charles Richard, J. L. *et al.* FACT Assists Base Excision Repair by Boosting the Remodeling Activity of RSC. *PLoS Genet.* **12**, e1006221 (2016).
34. Joseph, J. T. *et al.* Chromatin regulator HELLS mediates SSB repair and responses to DNA alkylation damage. *BioRxiv Prepr. Serv. Biol.* 2024.12.19.629292 (2025) doi:10.1101/2024.12.19.629292.
35. Gibbs-Seymour, I., Fontana, P., Rack, J. G. M. & Ahel, I. HPF1/C4orf27 Is a PARP-1-Interacting Protein that Regulates PARP-1 ADP-Ribosylation Activity. *Mol. Cell* **62**, 432–442 (2016).
36. Bonfiglio, J. J. *et al.* Serine ADP-Ribosylation Depends on HPF1. *Mol. Cell* **65**, 932-940.e6 (2017).
37. Smith, R. *et al.* HPF1-dependent histone ADP-ribosylation triggers chromatin relaxation to promote the recruitment of repair factors at sites of DNA damage. *Nat. Struct. Mol. Biol.* **30**, 678–691 (2023).
38. Kutuzov, M., Sayfullina, D., Belousova, E. & Lavrik, O. HPF1 Regulates Pol β Efficiency in Nucleosomes via the Modulation of Total Poly(ADP-Ribose) Synthesis. *Int. J. Mol. Sci.* **26**, 1794 (2025).
39. Smith, R., Sellou, H., Chapuis, C., Huet, S. & Timinszky, G. CHD3 and CHD4 recruitment and chromatin remodeling activity at DNA breaks is promoted by early poly(ADP-ribose)-dependent chromatin relaxation. *Nucleic Acids Res.* **46**, 6087–6098 (2018).
40. Mohapatra, J. *et al.* Serine ADP-ribosylation marks nucleosomes for ALC1-dependent chromatin remodeling. *eLife* **10**, e71502 (2021).
41. Pinto Jurado, E. *et al.* The recruitment of ACF1 and SMARCA5 to DNA lesions relies on ADP-ribosylation dependent chromatin unfolding. *Mol. Biol. Cell* **35**, br7 (2024).
42. Bacic, L. *et al.* Asymmetric nucleosome PARylation at DNA breaks mediates directional nucleosome sliding by ALC1. *Nat. Commun.* **15**, 1000 (2024).

646 43. Kurgina, T. A. *et al.* Dual function of HPF1 in the modulation of PARP1 and PARP2 activities.
647 *Commun. Biol.* **4**, 1259 (2021).
648 44. Ahel, D. *et al.* Poly(ADP-ribose)-dependent regulation of DNA repair by the chromatin remodeling
649 enzyme ALC1. *Science* **325**, 1240–1243 (2009).
650 45. Tsuda, M. *et al.* ALC1/CHD1L, a chromatin-remodeling enzyme, is required for efficient base excision
651 repair. *PloS One* **12**, e0188320 (2017).
652 46. Ramakrishnan, N. *et al.* Nucleolytic processing of abasic sites underlies PARP inhibitor
653 hypersensitivity in ALC1-deficient BRCA mutant cancer cells. *Nat. Commun.* **15**, 6343 (2024).
654 47. Meas, R. & Smerdon, M. J. Nucleosomes determine their own patch size in base excision repair. *Sci.*
655 *Rep.* **6**, 27122 (2016).
656 48. Niedergang, C. P., de Murcia, G., Ittel, M. E., Pouyet, J. & Mandel, P. Time course of polynucleosome
657 relaxation and ADP-ribosylation. Correlation between relaxation and histone H1 hyper-ADP-
658 ribosylation. *Eur. J. Biochem.* **146**, 185–191 (1985).
659 49. Li, Z. *et al.* Destabilization of linker histone H1.2 is essential for ATM activation and DNA damage
660 repair. *Cell Res.* **28**, 756–770 (2018).
661 50. Wu, D. & Piszczek, G. Standard protocol for mass photometry experiments. *Eur. Biophys. J. EBJ* **50**,
662 403–409 (2021).
663 51. Malanga, M., Atorino, L., Tramontano, F., Farina, B. & Quesada, P. Poly(ADP-ribose) binding
664 properties of histone H1 variants. *Biochim. Biophys. Acta* **1399**, 154–160 (1998).
665 52. Fahrer, J. *et al.* High-affinity interaction of poly(ADP-ribose) and the human DEK oncoprotein
666 depends upon chain length. *Biochemistry* **49**, 7119–7130 (2010).
667 53. Maltseva, E. A., Krasikova, Y. S., Sukhanova, M. V., Rechkunova, N. I. & Lavrik, O. I. Replication
668 protein A as a modulator of the poly(ADP-ribose)polymerase 1 activity. *DNA Repair* **72**, 28–38
669 (2018).
670 54. Moor, N. A., Vasil'eva, I. A., Anarbaev, R. O., Antson, A. A. & Lavrik, O. I. Quantitative
671 characterization of protein–protein complexes involved in base excision DNA repair. *Nucleic Acids*
672 *Res.* **43**, 6009–6022 (2015).
673 55. Lavrik, O. I. PARPs' impact on base excision DNA repair. *DNA Repair* **93**, 102911 (2020).
674 56. Vasil'eva, I. A., Moor, N. A. & Lavrik, O. I. Effect of Human XRCC1 Protein Oxidation on the
675 Functional Activity of Its Complexes with the Key Enzymes of DNA Base Excision Repair. *Biochem.*
676 *Biokhimiia* **85**, 288–299 (2020).
677 57. Lavrik, O. I. *et al.* Photoaffinity Labeling of Mouse Fibroblast Enzymes by a Base Excision Repair
678 Intermediate: EVIDENCE FOR THE ROLE OF POLY(ADP-RIBOSE) POLYMERASE-1 IN DNA REPAIR*. *J.*
679 *Biol. Chem.* **276**, 25541–25548 (2001).
680 58. McGinty, R. K. & Tan, S. Principles of nucleosome recognition by chromatin factors and enzymes.
681 *Curr. Opin. Struct. Biol.* **71**, 16–26 (2021).
682 59. Nagpal, A. *et al.* The zinc finger of DNA ligase 3α binds to nucleosomes via an arginine anchor. *Nat.*
683 *Commun.* **16**, 11531 (2025).
684 60. Vasil'eva, I., Moor, N., Anarbaev, R., Kutuzov, M. & Lavrik, O. Functional Roles of PARP2 in
685 Assembling Protein-Protein Complexes Involved in Base Excision DNA Repair. *Int. J. Mol. Sci.* **22**,
686 4679 (2021).
687 61. Rajendran, S., Jezewska, M. J. & Bujalowski, W. Recognition of template-primer and gapped DNA
688 substrates by the human DNA polymerase beta. *J. Mol. Biol.* **308**, 477–500 (2001).
689 62. Staynov, D. Z. & Crane-Robinson, C. Footprinting of linker histones H5 and H1 on the nucleosome.
690 *EMBO J.* **7**, 3685–3691 (1988).
691 63. Crane-Robinson, C. Where is the globular domain of linker histone located on the nucleosome?
692 *Trends Biochem. Sci.* **22**, 75–77 (1997).
693 64. Syed, S. H. *et al.* Single-base resolution mapping of H1-nucleosome interactions and 3D organization
694 of the nucleosome. *Proc. Natl. Acad. Sci. U. S. A.* **107**, 9620–9625 (2010).

695 65. Stone, P. R., Lorimer, W. S. & Kidwell, W. R. Properties of the complex between histone H1 and
696 poly(ADP-ribose synthesised in HeLa cell nuclei. *Eur. J. Biochem.* **81**, 9–18 (1977).
697 66. Bartolomei, G., Leutert, M., Manzo, M., Baubec, T. & Hottiger, M. O. Analysis of Chromatin ADP-
698 Ribosylation at the Genome-wide Level and at Specific Loci by ADPr-ChAP. *Mol. Cell* **61**, 474–485
699 (2016).
700 67. Strickfaden, H. *et al.* Poly(ADP-ribosyl)ation-dependent Transient Chromatin Decondensation and
701 Histone Displacement following Laser Microirradiation. *J. Biol. Chem.* **291**, 1789–1802 (2016).
702 68. Cistulli, C., Lavrik, O. I., Prasad, R., Hou, E. & Wilson, S. H. AP endonuclease and poly(ADP-ribose)
703 polymerase-1 interact with the same base excision repair intermediate. *DNA Repair* **3**, 581–591
704 (2004).
705 69. Farrés, J. *et al.* PARP-2 sustains erythropoiesis in mice by limiting replicative stress in erythroid
706 progenitors. *Cell Death Differ.* **22**, 1144–1157 (2015).
707 70. Lin, X. *et al.* PARP inhibitors trap PARP2 and alter the mode of recruitment of PARP2 at DNA damage
708 sites. *Nucleic Acids Res.* **50**, 3958–3973 (2022).
709 71. Lin, X. *et al.* Inactive Parp2 causes Tp53-dependent lethal anemia by blocking replication-associated
710 nick ligation in erythroblasts. *Mol. Cell* **84**, 3916-3931.e7 (2024).
711 72. Amé, J.-C., Kalisch, T., Dantzer, F. & Schreiber, V. Purification of recombinant poly(ADP-ribose)
712 polymerases. *Methods Mol. Biol.* **780**, 135–152 (2011).
713 73. Strauss, P. R., Beard, W. A., Patterson, T. A. & Wilson, S. H. Substrate binding by human
714 apurinic/apyrimidinic endonuclease indicates a Briggs-Haldane mechanism. *J. Biol. Chem.* **272**,
715 1302–1307 (1997).
716 74. Nazarkina, J. K., Petrousseva, I. O., Safronov, I. V., Lavrik, O. I. & Khodyreva, S. N. Interaction of Flap
717 Endonuclease-1 and Replication Protein A with Photoreactive Intermediates of DNA Repair.
718 *Biochem. Mosc.* **68**, 934–942 (2003).
719 75. Kumar, A. *et al.* Studies of the domain structure of mammalian DNA polymerase beta. Identification
720 of a discrete template binding domain. *J. Biol. Chem.* **265**, 2124–2131 (1990).
721 76. Krasikova Y. *et al.* Does the XPA-FEN1 Interaction Concern to Nucleotide Excision Repair or Beyond?
722 *Biomolecules*. **14**, 814 (2024).
723 77. Kutuzov, M., Kurgina, T., Belousova, E., Khodyreva, S. & Lavrik, O. Optimization of nucleosome
724 assembly from histones and model DNAs and estimation of the reconstitution efficiency. *Biopolym.*
725 *Cell* **35**, 91–98 (2019).
726 78. Sidorov, G. V., Zverkov, Yu. B., Shram, S. I., Lazurkina, T. Yu. & Myasoedov, N. F. Chemical and
727 enzymatic synthesis of tritium labelled coenzymes. *J. Label. Compd. Radiopharm.* **46**, 465–473
728 (2003).
729 79. Lowary, P. T. & Widom, J. New DNA sequence rules for high affinity binding to histone octamer and
730 sequence-directed nucleosome positioning. *J. Mol. Biol.* **276**, 19–42 (1998).
731 80. Kurgina, T. A., Anarbaev, R. O., Sukhanova, M. V. & Lavrik, O. I. A rapid fluorescent method for the
732 real-time measurement of poly(ADP-ribose) polymerase 1 activity. *Anal. Biochem.* **545**, 91–97
733 (2018).